Empa
Materials Science and Technology

Postprint

This is the accepted version of a paper published in *J. Am. Chem. Soc.*
This paper has been peer-reviewed but does not include the final publisher proof-corrections or journal pagination.

Citation for the original published paper (version of record):

Xiao-Ye Wang, Thomas Dienel, Marco Di Giovannantonio, Gabriela Borin Barin, Neerav Kharche, Okan Deniz, José I. Urgel, Roland Widmer, Samuel Stolz, Luis Henrique De Lima, Matthias Muntwiler, Matteo Tommasini, Vincent Meunier, Pascal Ruffieux, Xinliang Feng, Roman Fasel, Klaus Müllen, and Akimitsu Narita

On-surface Synthesis of Atomically Precise Graphene Nanoribbons

J. Am. Chem. Soc. 139, 4671-4674 (2017)

https://doi.org/10.1021/jacs.7b02258

Access to the published version may require subscription.

N.B. When citing this work, please cite the original published paper.

Heteroatom-Doped Perihexacene from a Double Helicene Precursor: On-Surface Synthesis and Properties

Xiao-Ye Wang,[†§] Thomas Dienel,[‡§] Marco Di Giovannantonio,[‡] Gabriela Borin Barin,[‡] Neerav Kharche,[⊥] Okan Deniz,[‡] José I. Urgel,[‡] Roland Widmer,[‡] Samuel Stolz,[‡] Luis Henrique De Lima,[⊤] Matthias Muntwiler,[⊤] Matteo Tommasini,[#] Vincent Meunier,[⊥] Pascal Ruffieux,[‡] Xinliang Feng,[∥] Roman Fasel,*[‡▽] Klaus Müllen,*[†] Akimitsu Narita*[†]

[†] Max Planck Institute for Polymer Research, Ackermannweg 10, 55128 Mainz, Germany

[‡] Empa, Swiss Federal Laboratories for Materials Science and Technology, 8600 Dübendorf, Switzerland

[⊥] Department of Physics, Rensselaer Polytechnic Institute, Troy, 12180 New York, USA

[⊤] Paul Scherrer Institut, 5232 Villigen PSI, Switzerland

[#] Dipartimento di Chimica, Materiali ed Ingegneria Chimica 'G. Natta', Politecnico di Milano, Piazza Leonardo da Vinci 32, 20133 Milano, Italy

[∥] Center for Advancing Electronics Dresden, Department of Chemistry and Food Chemistry, Technische Universität Dresden, 01062 Dresden, Germany

[▽] Department of Chemistry and Biochemistry, University of Bern, 3012 Bern, Switzerland

Supporting Information Placeholder

ABSTRACT: We report on the surface-assisted synthesis and spectroscopic characterization of the hitherto longest periacene analogue with oxygen-boron-oxygen (OBO) segments along the zigzag edges, that is, a heteroatom-doped perihexacene **1**. Surface-catalyzed cyclodehydrogenation successfully transformed the double helicene precursor **2**, *i.e.* 12a,26a-dibora-12,13,26,27-tetraoxa-benzo[1,2,3-*hi*:4,5,6-*h'i'*]dihexacene, into the planar perihexacene analogue **1**, which was visualized by scanning tunneling microscopy (STM) and noncontact atomic force microscopy (nc-AFM). X-ray photoelectron spectroscopy, Raman spectroscopy, together with theoretical modeling, on both precursor **2** and product **1,** provided further insights into the cyclodehydrogenation process. Moreover, the nonplanar precursor **2** underwent a conformational change upon adsorption on surfaces, and one-dimensional self-assembled superstructures were observed for both **2** and **1** due to the presence of OBO units along the zigzag edges.

Periacenes, which comprise two laterally *peri*-fused linear acenes, are rectangular polycyclic aromatic hydrocarbons (PAHs) with both armchair and zigzag edges.[1] Theoretical investigation revealed their intriguing electronic and magnetic properties, which can be modulated by varying their molecular size.[2] However, experimentally studied periacenes are mostly perylenes and bisanthenes,[3] while the pursuit of longer periacenes, *i.e.* peritetracene and higher homologues, has been severely hampered by their poor stability.[4] In 2015, Rogers *et al.* synthesized peripentacene under ultrahigh vacuum (UHV) on a metal surface, which is to date the highest periacene reported in the literature.[5] On the other hand, we achieved heteroatom-doped peritetracenes in solution, providing a new type of periacene analogues with modified properties and excellent stability.[6] The synthesis of higher periacenes or their heteroanalogues has remained elusive.

Modern on-surface chemistry has expanded the synthetic toolbox of graphene nanostructures,[7] *e.g.* nanoscale PAHs (nanographene molecules) and graphene nanoribbons, and provided a new way to characterize the structures in addition to the conventional solution approach.[8] Properties of molecules confined on a surface have attracted significant interest. For example, molecular conformations can be affected by surfaces and by intermolecular interactions,[9] and molecules on surfaces can self-assemble into ordered supramolecular nanoarchitectures.[10] Such studies are fundamentally important for understanding the molecule-molecule and molecule-substrate interactions and eventually for designing a programmable assembly of molecules.[11]

Herein, we report on the synthesis of the first heteroatom-doped perihexacene **1**, the hitherto longest periacene analogue (~1.5 nm) with OBO segments on the zigzag edges (Scheme 1), via surface-assisted cyclodehydrogenation of a solution-synthesized precursor **2** on the Au(111) surface under UHV conditions. The precursor **2**, namely 12a,26a-dibora-12,13,26,27-tetraoxa-benzo[1,2,3-*hi*:4,5,6-*h'i'*]dihexacene, is indeed a π-extended double [5]helicene featuring nonplanarity and structural flexibility.[12] To our knowledge, the behavior of double helicenes on surfaces has never been investigated, compared with the well-studied monohelicenes.[13] The conformation of precursor **2** is revealed to be highly influenced by the metal surface and the self-assembly structures. Moreover, both precursor **2** and perihexacene analogue **1** form one-dimensional (1D) superstructures on surfaces by virtue of OBO units.

The synthesis of precursor **2** and perihexacene analogue **1** is depicted in Scheme 1. First, 2-methoxynaphthalene (**3**) was lithiated and then brominated by 1,2-dibromoethane to afford 2-bromo-3-methoxynaphthalene (**4**) in 74% yield. Subsequently, **4** was transformed to a Grignard reagent and reacted with hexabromobenzene (HBB). After quenching by I_2, 1,4-diiodo-2,3,5,6-tetra(3-methoxynaphthalen-2-yl)benzene (**5**) was obtained in 26% yield. Then, compound **5** was subjected to

lithiation and trapped by BBr_3 in chlorobenzene (CB). This intermediate subsequently underwent demethylative cyclization[14] at 40 °C to provide compound **2** in 43% yield. The oxidative cyclodehydrogenation of **2** was initially attempted in solution, using $FeCl_3$ or 2,3-dichloro-5,6-dicyano-1,4-benzoquinone (DDQ) as oxidants, which all resulted in mixtures of undefined products. Nevertheless, the cyclodehydrogenation of compound **2** was successfully achieved on Au(111) by heating the precursor at 380 °C, yielding the OBO-doped perihexacene **1**. The detailed on-surface conditions and characterizations will be discussed later.

Scheme 1. Synthetic route to perihexacene analogue 1.

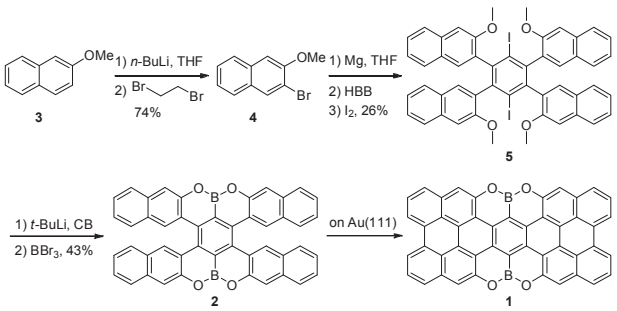

Considering the flexible conformations of double [5]helicenes,[6,14] we therefore carried out DFT calculations to investigate the favorable molecular conformation of double helicene **2**. As illustrated in Figure 1, in the gas phase, the twisted (T) conformation of **2** is thermodynamically more stable by 0.18 eV (4.15 kcal/mol) compared to the *anti*-folded (A) conformation. The isomerization barrier from T to A calculated by the nudged-elastic-band (NEB) method[15] is 1.13 eV (26.1 kcal/mol). These results are in good agreement with the quantum chemistry calculations at the B3LYP/6-311G(d,p) level, which estimated that T is more stable by 0.24 eV (5.6 kcal/mol) than A (Figure S6). These theoretical investigations indicate that compound **2** dominantly adopts the twisted conformation in the gas phase.

When precursor **2** was thermally sublimed under UHV onto an Au(111) substrate held at room temperature, the molecules self-assembled into well-ordered linear chains that followed the herringbone reconstruction of the gold substrate (Figure S2a). A closer inspection into the scanning tunneling microscopy (STM) images reveals that the building blocks of the assembled chains are dimers of compound **2**. The monomers mainly adopt the A conformation (Figure 2a), where the lifted parts face each other within each dimer (monomer distances projected along the chain are I = 1.1 nm (within dimers) and II = 1.2 nm (between dimers), model in Figure 2b). The assembly along the chain seems to be stabilized by O···H hydrogen bonds (dotted lines in Figure 2b). Occasionally, compound **2** can be found in the T conformation (7% of 265 molecules), without affecting the packing along the chain (one T molecule indicated by blue arrows in Figure 2a and b). To elucidate the predominant occurrence of monomers in the A conformation, molecule-substrate and molecule-molecule interactions have to be considered. We investigated the energies of both T and A conformations when supported on the Au(111) surfaces (Figure 1e). In contrast to the gas-phase properties, the relative energy of A is reduced on the surface, resulting in a slightly lower energy of about 0.03 eV (0.69 kcal/mol) compared to T. This change in the relative stability is also reflected in the fact that A has a higher substrate-binding energy compared to T (Table S2), implying that the substrate stabilizes the A conformation. Furthermore, when the hydrogen-bonded chains of precursor **2** (as shown in Figure 2a) are taken into account, the energy difference between A and T is more profound (Table S3). On the surface, A-chains become more stable compared to T-chains by 0.15 eV per molecule (in the gas phase, T-chains are more stable than A-chains by 0.30 eV per molecule). It is found that the substrate not only stabilizes A as a single molecule, but also stabilizes the H-bonds in the A-chains, resulting in the predominance of A on the surface.

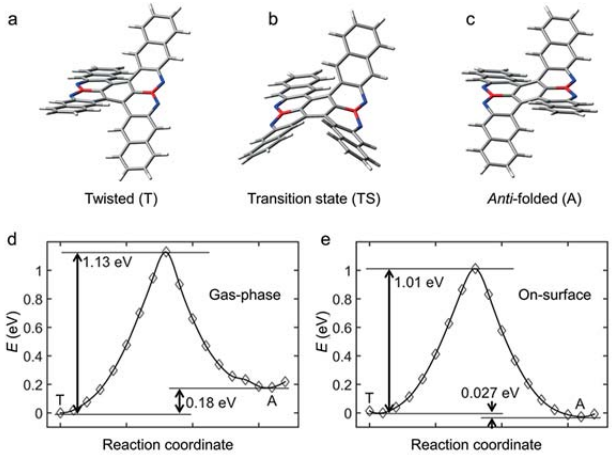

Figure 1. (a-c) DFT-optimized molecular geometries of the twisted and *anti*-folded **2** and the transition state from T to A. (d) Gas-phase and (e) on-surface energy barriers for the transformation from T to A calculated by the nudged-elastic-band (NEB) method.

The synthesis of the planarized perihexacene analogue **1** was further achieved by thermally annealing the substrate at 380 °C (Figure 2d and S2b). The alternating assembly of compound **2** into well-reproduced dimers is replaced by a random sequence of uniform and meandering sections along the chain. The latter is based on the O···H hydrogen bonds with lengths of about 1.9 Å (monomer distance IV = 1.04 nm, Figures 2f and S3d). Contrarily, the abreast assembly reveals facing OBO units of neighboring molecules, which could host a coordinating metal atom (monomer distance III = 1.13 nm, Figures 2e and S3e). The coordinating atoms are presumably gold adatoms that are occasionally imaged in STM (indicated by a green arrow in Figure 2d).[16] The self-assembly behavior of perihexacene analogue **1** is distinct from that of the hydrocarbon-based peripentacene, which spreads discretely on the surface.[5] This observation indicates that such intermolecular interactions resulting from heteroatoms on the edges can be potentially exploited for fabricating ordered graphene nanostructures.[17] In order to unambiguously clarify the structure of **1**, noncontact atomic force microscopy (nc-AFM) with CO-functionalized tips was performed, which provides ultimate resolution at the single bond level.[18] The perihexacene skeleton of **1** can be clearly visualized in Figure 2g (overlaid structural model in Figure 2h).

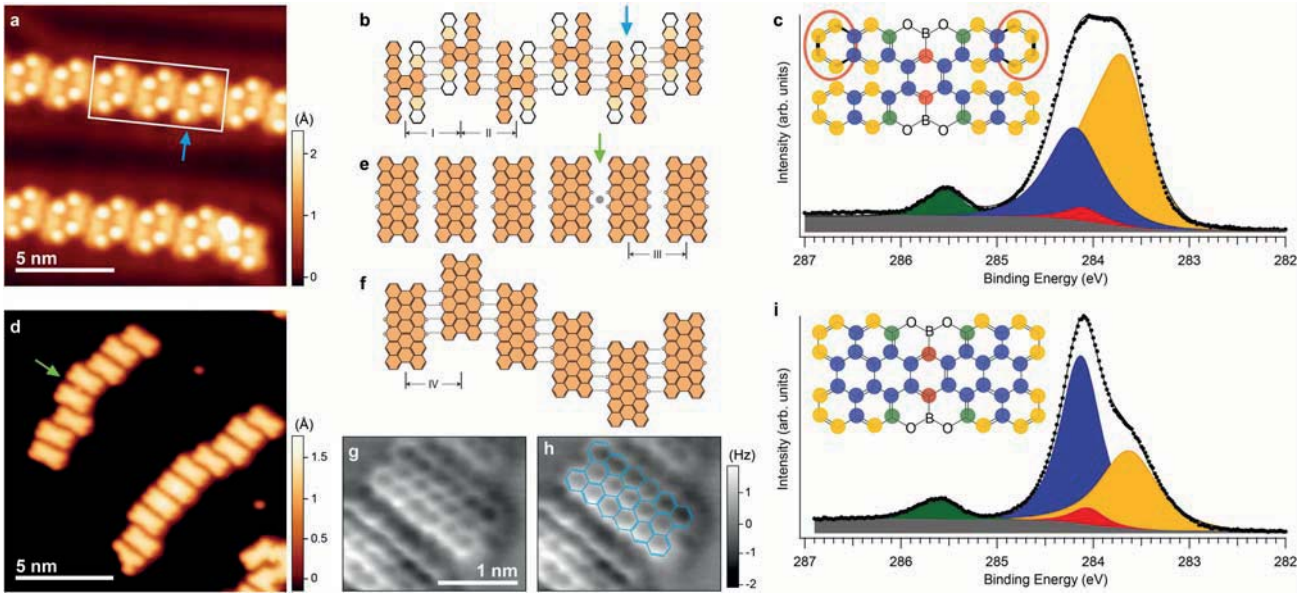

Figure 2. On-surface reaction of precursor **2** to perihexacene analogue **1**. (a) STM image of precursor **2** deposited on Au(111) held at room temperature (tunneling parameters: −1.76 V, 100 pA; blue arrow at T conformation). (b) Schematic representation of the assembly of precursor **2** (three dimers) within the white rectangle in (a). Dotted lines indicate O···H hydrogen bonds; darker parts correspond to lower parts of the molecules near the surface; the blue arrow indicates a monomer in T conformation. (c) High-resolution XPS spectrum of the C 1s level of **2** on Au(111) at room temperature. Red circles indicate the lifted parts of the molecule. (d) STM image of product **1** after annealing to 380 °C (green arrow to Au adatom; tunneling parameters: 1.2 V, 20 pA). (e) Schematic representation of the abreast molecular assembly (grey dot representing an occasional Au adatom). (f) Structure model of the self-assembly based on O···H hydrogen bonds (indicated by dotted lines). (g,h) Frequency shift images with CO-sensitized tips (nc-AFM, measured at constant height, structural model overlaid in h). (i) High-resolution XPS spectrum after annealing at 430 °C. A Shirley background has been adopted to fit the XPS data and the colors of the four fitting Voigt functions correspond to those of the dots in the molecular skeleton (c, i).

Complementary information on the cyclodehydrogenation is provided by X-ray photoelectron spectroscopy (XPS). The high-resolution XPS measurements before and after the annealing show different features of the C 1s spectra, indicating the chemical transformation from *anti*-folded **2** to perihexacene analogue **1** upon thermal annealing. The A conformation of **2** leads to different heights of the atoms with respect to the surface, particularly the carbon atoms responsible for the C−H signal (orange dots in Figure 2c and i). Because of a different screening effect from the surface, the binding energy of the atoms away from the surface is higher than the expected value. We addressed this behavior by using an asymmetric Voigt component in the fit (Figure 2c). After thermal annealing, however, all the atoms of the planarized molecule lie at the same height, so only symmetric Voigt functions were used. Before and after raising the temperature, the C−O and C−B signals did not change much, but the C−C component increased and C−H part decreased, in line with the expected change of the ratio C−C : C−H from 2 : 3 to 3 : 2. This result again corroborates the successful cyclodehydrogenation upon thermal annealing. To gain deeper insight into the cyclodehydrogenation process, a fast-XPS map at the C 1s level was acquired during the temperature increase (one C 1s spectrum every 5 s, Figure S5). The linear profiles as a function of the annealing temperature revealed a gradual cyclodehydrogenation starting at about 200 °C and completing at about 380 °C. Above 380 °C, the spectra barely changed. The total area of each C 1s spectrum as a function of the temperature indicated that no significant desorption of the molecules from the surface took place during the annealing process.

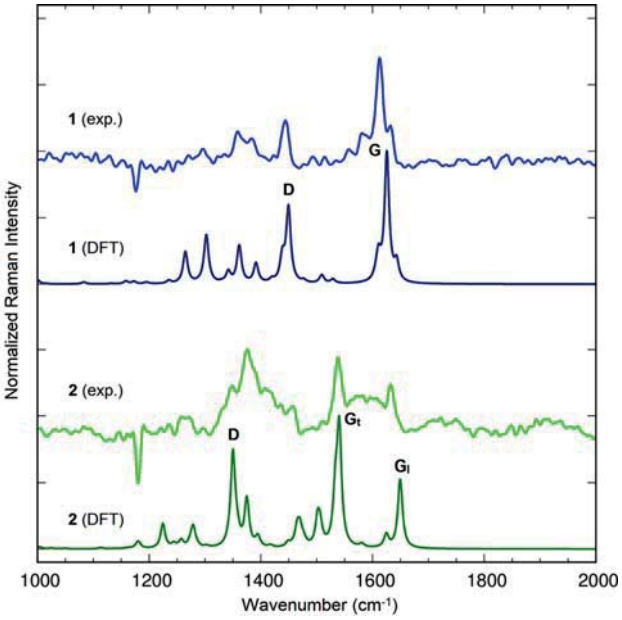

Figure 3. Experimental and DFT-simulated Raman spectra of **1** (light and dark blue) and **2** (light and dark green). G_t and G_l are the G modes of **2** occurring along the transversal and longitudinal axes of the molecule. The G mode of **1** is longitudinal.

Raman analysis of precursor **2** and perihexacene analogue **1** was performed on the Au(111) surface with an excitation wavelength of 532 nm (2.33 eV), displaying completely different spectra for the two samples (Figure 3). The experimental results are in good agreement with the DFT-simulated spectra, further confirming the successful formation of perihexacene analogue **1**. As expected for both **1** and **2**, the characteristic G and D Raman signals of graphene molecules,[19]

which is due to confinement of π electrons in finite size, can be assigned in the experimental spectra based on DFT calculations. In particular, for molecule **1** the G and D lines are observed at 1612 cm^{-1} and 1443 cm^{-1}, respectively. For molecule **2** the G line displays both a longitudinal component (G_l, 1634 cm^{-1}) and a transversal component (G_t, 1537 cm^{-1}) and the D line is observed at 1373 cm^{-1} (see the Supporting Information for details).

In summary, we have achieved on-surface synthesis and characterization of heteroatom-doped perihexacene **1**, the longest periacene analogue to date. The successful synthesis of **1** was unambiguously revealed by STM and nc-AFM and further characterized by XPS and Raman spectroscopy. Moreover, the on-surface behavior of a double helicene has been investigated for the first time. It is interesting to find that the preferred conformation of the double helicene precursor **2** was influenced upon adsorption on surfaces. Furthermore, both **2** and **1** self-assembled into 1D superstructures through hydrogen bonding and/or metal coordination at the OBO units on the edges. This work demonstrates a potential heteroatom-doping strategy of the edges for fabricating tailor-made graphene nanoarchitectures, and highlights the importance of combining in-solution and on-surface chemistry to pursue a further variety of nanographene structures.

ASSOCIATED CONTENT

Supporting Information

The Supporting Information is available free of charge on the ACS Publications website.
Experimental details and data, theoretical simulations (PDF).

AUTHOR INFORMATION

Corresponding Author

*muellen@mpip-mainz.mpg.de
*roman.fasel@empa.ch
*narita@mpip-mainz.mpg.de

Author Contributions

[§]These authors contributed equally.

Notes

The authors declare no competing financial interests.

ACKNOWLEDGMENT

We acknowledge the financial support from Max Planck Society and European Commission through the FET-Proactive Project "MoQuaS", contract N.610449, the Graphene Flagship and the Swiss National Science Foundation. The XPS experiments were performed on the X03DA (PEARL) beamline at the Swiss Light Source, Paul Scherrer Institut, Villigen, Switzerland. Lukas Rotach is acknowledged for technical support. Xiao-Ye Wang is grateful for the fellowship from Alexander von Humboldt Foundation.

REFERENCES

(1) (a) Sun, Z.; Ye, Q.; Chi, C.; Wu, J. *Chem. Soc. Rev.* **2012**, *41*, 7857. (b) Ye, Q.; Chi, C. *Chem. Mater.* **2014**, *26*, 4046.
(2) (a) Jiang, D.-E.; Dai, S. *Chem. Phys. Lett.* **2008**, *466*, 72. (b) Moscardó, F.; San-Fabián, E. *Chem. Phys. Lett.* **2009**, *480*, 26.
(3) (a) Fort, E. H.; Donovan, P. M.; Scott, L. T. *J. Am. Chem. Soc.* **2009**, *131*, 16006. (b) Fort, E. H.; Scott, L. T. *Angew. Chem. Int. Ed.* **2010**, *49*, 6626. (c) Li, J.; Zhang, K.; Zhang, X.; Huang, K.-W.; Chi, C.; Wu, J. *J. Org. Chem.* **2010**, *75*, 856.
(4) (a) Zöphel, L.; Berger, R.; Gao, P.; Enkelmann, V.; Baumgarten, M.; Wagner, M.; Müllen, K. *Chem. Eur. J.* **2013**, *19*, 17821. (b) Liu, J.; Ravat, P.; Wagner, M.; Baumgarten, M.; Feng, X.; Müllen, K. *Angew. Chem. Int. Ed.* **2015**, *54*, 12442. (c) Zhang, X.; Li, J.; Qu, H.; Chi, C.; Wu, J. *Org. Lett.* **2010**, *12*, 3946.
(5) Rogers, C.; Chen, C.; Pedramrazi, Z.; Omrani, A. A.; Tsai, H.-Z.; Jung, H. S.; Lin, S.; Crommie, M. F.; Fischer, F. R. *Angew. Chem. Int. Ed.* **2015**, *54*, 15143.
(6) Wang, X.-Y.; Narita, A.; Zhang, W.; Feng, X.; Müllen, K. *J. Am. Chem. Soc.* **2016**, *138*, 9021.
(7) (a) Treier, M.; Pignedoli, C. A.; Laino, T.; Rieger, R.; Müllen, K.; Passerone, D.; Fasel, R. *Nature Chem.* **2011**, *3*, 61. (b) Palma, C.-A.; Samori, P. *Nature Chem.* **2011**, *3*, 431. (c) Narita, A.; Wang, X.-Y.; Feng, X.; Müllen, K. *Chem. Soc. Rev.* **2015**, *44*, 6616. (d) Talirz, L.; Ruffieux, P.; Fasel, R. *Adv. Mater.* **2016**, *28*, 6222.
(8) Pavliček, N.; Gross, L. *Nature Rev. Chem.* **2017**, *1*, 0005.
(9) (a) Stöckl, Q. S.; Hsieh, Y.-C.; Mairena, A.; Wu, Y.-T.; Ernst, K.-H. *J. Am. Chem. Soc.* **2016**, *138*, 6111. (b) Weigelt, S.; Busse, C.; Petersen, L.; Rauls, E.; Hammer, B.; Gothelf, K. V.; Besenbacher, F.; Linderoth, T. R. *Nature Mater.* **2006**, *5*, 112.
(10) (a) Kudernac, T.; Lei, S.; Elemans, J. A. A. W.; De Feyter, S. *Chem. Soc. Rev.* **2009**, *38*, 402. (b) Mali, K. S.; Adisoejoso, J.; Ghijsens, E.; De Cat, I.; De Feyter, S. *Acc. Chem. Res.* **2012**, *45*, 1309. (c) Slater, A. G.; Perdigão, L. M. A.; Beton, P. H.; Champness, N. R. *Acc. Chem. Res.* **2014**, *47*, 3417. (d) Otero, R.; Gallego, J. M.; de Parga, A. L. V.; Martín, N.; Miranda, R. *Adv. Mater.* **2011**, *23*, 5148.
(11) (a) Bouju, X.; Mattioli, C.; Franc, G.; Pujol, A.; Gourdon, A. *Chem. Rev.* **2017**, *117*, 1407. (b) Kühnle, A. *Curr. Opin. Colloid Interface Sci.* **2009**, *14*, 157.
(12) Shen, Y.; Chen, C.-F. *Chem. Rev.* **2012**, *112*, 1463.
(13) Ernst, K.-H. *Acc. Chem. Res.* **2016**, *49*, 1182.
(14) Katayama, T.; Nakatsuka, S.; Hirai, H.; Yasuda, N.; Kumar, J.; Kawai, T.; Hatakeyama, T. *J. Am. Chem. Soc.* **2016**, *138*, 5210.
(15) Henkelman, G.; Uberuaga, B. P.; Jónsson, H. *J. Chem. Phys.* **2000**, *113*, 9901.
(16) (a) Lin, N.; Stepanow, S.; Ruben, M.; Barth, J. V. In *Templates in Chemistry III*; Broekmann, P., Dötz, K.-H., Schalley, C. A., Eds.; Springer Berlin Heidelberg: 2009, p 1. (b) Barth, J. V. *Annu. Rev. Phys. Chem.* **2007**, *58*, 375.
(17) Cai, J.; Pignedoli, C. A.; Talirz, L.; Ruffieux, P.; Söde, H.; Liang, L.; Meunier, V.; Berger, R.; Li, R.; Feng, X.; Müllen, K.; Fasel, R. *Nature Nanotechnol.* **2014**, *9*, 896.
(18) (a) Gross, L.; Mohn, F.; Moll, N.; Liljeroth, P.; Meyer, G. *Science* **2009**, *325*, 1110. (b) Gross, L.; Mohn, F.; Moll, N.; Schuler, B.; Criado, A.; Guitián, E.; Peña, D.; Gourdon, A.; Meyer, G. *Science* **2012**, *337*, 1326.
(19) (a) Castiglioni, C.; Tommasini, M.; Zerbi, G. *Phil. Trans. R. Soc. Lond. A* **2004**, *362*, 2425. (b) Maghsoumi, A.; Brambilla, L.; Castiglioni, C.; Müllen, K.; Tommasini, M. *J. Raman Spectrosc.* **2015**, *46*, 757.

Table of Contents Graphic